Journal of the Optical Society of America B

OPTICAL PHYSICS

Dynamics of nonclassical properties of a SU(3) system interacting with two open parametric amplifier modes

A.-B. A. Mohamed,[1,2,*] H. A. Hessian,[2,3] A.-S. F. Obada,[4] and H. Eleuch[5,6]

[1]Department of Mathematics, College of Science and Humanities in Al-Aflaj, Prince Sattam Bin Abdulaziz University, Al-Kharj, Saudi Arabia
[2]Department of Mathematics, Faculty of Science, Assiut University, Assiut, Egypt
[3]Faculty of Science, Al-Baha University, Al-Baha, Saudi Arabia
[4]Department of Mathematics, Faculty of Science, Al-Azhar University, Nasr City 11884, Cairo, Egypt
[5]Department of Applied Physics and Astronomy, University of Sharjah, Sharjah, United Arab Emirates
[6]Institute for Quantum Science and Engineering, Texas A&M University, College Station, Texas 77843, USA
*Corresponding author: abdelbastm@aun.edu.eg

Received 23 October 2020; revised 14 March 2021; accepted 21 March 2021; posted 23 March 2021 (Doc. ID 413137); published 16 April 2021

We introduce an analytical description of an open bimodal cavity containing a Λ-type three-level atom. We explore the effect of the atom–cavity nonlinear interaction, the cavity dissipation, and the initial coherent intensity on the dynamics of the nonclassical correlations for a cavity prepared initially in a superposition of nonlinear coherent states. The nonlinear interaction generates a regular entanglement between the subsystems, and populates the energy atomic states. We show that the collapse phenomenon is a good indicator of the generated quantum coherence. The growth of the entropy is used to explore the generated entanglement (if the dissipation is absent) and mixedness (in the presence of the dissipation). It is found that the generation and the robustness of the quantum synchronization and the correlations between the subsystems are very sensitive to the dissipation, the superposition, and the coherent intensity of the initial Barut–Girardello coherent states.

https://doi.org/10.1364/JOSAB.413137

1. INTRODUCTION

The study of quantum coherence, entanglement, and purity loss, in cavity quantum electrodynamics (QED), has substantially progressed [1,2]. Recently, entanglement, quantum coherence, and transition energy have become active research themes due to their role as essential resources for quantum information [3,4], in particular for quantum teleportation [5], dense coding [6], cryptography [7], and computation [8].

It is well-known that quantum coherence is very sensitive to the decoherence and dissipation resources, which lead to the transit of quantum systems to classical systems. The exploration of the dissipation effects on the nonlinear interactions between the multilevel atomic system and cavity fields was limited [9–14].

The nonlinear atom–cavity interactions induce remarkable changes in the dynamical properties of the system. They can be realized in different real systems as trapped ions [15] and superconducting circuits [16,17]. The atom–cavity interaction is usually described by the Jaynes–Cummings model (JC model) [18]. Its generalization models are applied to the interaction between multilevel atoms and a multimode cavity [19], multiphoton transitions, and a Kerr-like medium [20].

The three-level atomic systems with cavity systems provide more secure quantum key distributions [21,22] than those based on two-level systems [23,24]. In addition, channel capacity and security in the quantum-based teleportation protocols can be enhanced using SU(3) systems [25]. SU(3) systems can be realized based on the superconductor circuits [26], nitrogen-vacancy centers [27], and quantum dot molecules [28]. The interaction between a Λ-type SU(3) system and cavity fields has several contributions in quantum information, such as generation of long-living entanglement [29,30] controlling visibility and distinguishability of interference and diffraction patterns [31], simulation of the emission of a single-photon pulse [32], and population transfer [33].

The entangled Barut–Girardello coherent state (BGCS) [34] is of particular importance for quantum processing [35]. The entangled pair-coherent states [36,37] and the BCGSs are realized experimentally [38].

Previous investigations dealt with generated Λ-type atom-cavity entanglement in different cavities. For examples, we can mention studies on: dissipative vacuum cavities coupled to non-Markovian environments [29], bimodal photons in a thermal optical cavity [30], a closed vacuum cavity with two field modes [39], a closed one-mode cavity field with both classical gravity and quantum radiation [40], and a closed two-mode cavity field with nondegenerate two-photon transitions with intensity-dependent coupling [41].

In this paper, based on the population inversion, entropy, and negativity, we investigate the dynamics of the quantum coherence (entanglement/mixedness) for a Λ-type three-level atom interacting with an open parametric amplifier coherent cavity modes. The cavity modes are initially in a superposition of Barut–Girardello coherent states. This paper has four sections. In Section 2, we present the model of the SU(1,1)–SU(3) system and solve analytically the master equation. In Section 3, the quantum coherence quantifiers and their dynamics, respectively, are introduced and investigated. Finally, we finish with the conclusion in Section 4.

2. DESCRIPTION OF THE MODEL

Here, we consider a Λ-type three-level atom interacting with an open parametric amplifier cavity through nondegenerate two-photon processes. The model's Hamiltonian, after applying rotating wave approximations, is given by $\hat{H}=\hat{H}_0+\hat{H}_{\mathrm{int}}$, where

$$\hat{H}_0=\sum_{i=1,2}\omega_i(\hat{a}_i^\dagger\hat{a}_i+\frac{1}{2})+\sum_{k=e,g,f}\omega_k|k\rangle\langle k|, \tag{1}$$

$$\begin{aligned}\hat{H}_{\mathrm{int}}=&\lambda_1(\hat{a}_1\hat{a}_2|e\rangle\langle g|+\hat{a}_1^\dagger\hat{a}_2^\dagger|g\rangle\langle e|)\\&+\lambda_2(\hat{a}_1\hat{a}_2|e\rangle\langle f|+\hat{a}_1^\dagger\hat{a}_2^\dagger|f\rangle\langle e|),\end{aligned} \tag{2}$$

where $\hat{a}_1(\hat{a}_1^\dagger)$ and $\hat{a}_2(\hat{a}_2^\dagger)$ are the annihilation (creation) operators for the field modes. The $\omega_k(i=e,g,f)$ are the atomic frequencies of the upper state $|a\rangle$ and two lower states, $|g\rangle$ and $|f\rangle$. The $|i\rangle\langle j|$, $(i,j=e,g,f)$ are the projection operators of the Λ-type qutrit, and λ_1 and λ_2 are the coupling constants for the $|e\rangle\leftrightarrow|g\rangle$ and $|e\rangle\leftrightarrow|f\rangle$ transitions, respectively. The Λ-qutrit can be experimentally implemented with the nitrogen-vacancy centers [42] and superconducting circuits [43,44]. The interaction of a pair of parametric amplifiers cavity fields was realized with atoms coupled to resonator modes [45]. Two-photon interferences with degenerate and nondegenerate paired photons were conceived experimentally from spontaneous four-wave mixing in the three-level cold atom [46].

For the case $\omega_1=\omega_2=\omega$, the Hamiltonian $\hat{H}_0$ in term the atomic probability, $\hat{I}=|e\rangle\langle e|+|g\rangle\langle g|+|f\rangle\langle f|$, and the excitation number, $\hat{N}=\hat{a}_1^\dagger\hat{a}_1+\hat{a}_2^\dagger\hat{a}_2+|e\rangle\langle e|$, can be rewritten as [47]

$$\hat{H}_0=\omega(\hat{N}+1)+(\omega_e-\omega)\hat{I}-\delta_g|g\rangle\langle g|-\delta_f|f\rangle\langle f|, \tag{3}$$

where $\delta_g=(\omega_e-\omega_g)-\omega$ and $\delta_f=(\omega_e-\omega_f)-\omega$. If we take $-\delta_g=\delta_f=\delta$, then $\omega=\omega_e-\frac{1}{2}(\omega_g+\omega_f)$, and the detuning of the field is given by $\delta=\frac{1}{2}(\omega_g-\omega_f)$. By using SU(1, 1) Lie algebra operators [48,49], $\hat{S}_0$ and $\hat{S}_\pm$, the Hamiltonian of the system can be rewritten as

$$\begin{aligned}\hat{H}=&(\hat{S}_0+|e\rangle\langle e|)\omega+\delta(|g\rangle\langle g|-|f\rangle\langle f|)+\lambda_1(\hat{S}_-|e\rangle\langle g|)\\&+\hat{S}_+|g\rangle\langle e|+\lambda_2(\hat{S}_-|e\rangle\langle f|+\hat{S}_+|f\rangle\langle e|),\end{aligned} \tag{4}$$

where $\hat{S}_0=\hat{a}_1^\dagger\hat{a}_1+\hat{a}_2^\dagger\hat{a}_2+1$, and $\hat{S}_+=\hat{a}_1^\dagger\hat{a}_2^\dagger=\hat{S}_-^\dagger$ satisfy $[\hat{S}_0,\hat{S}_\pm]=\pm\hat{S}_\pm$, $[\hat{S}_-,\hat{S}_+]=2\hat{S}_0$. Here, we focus on the resonant case $(\delta=0)$.

The Hamiltonian in Eq. (4) represents the interaction between the SU(1, 1) and SU(3) systems. The $\hat{S}_0$ and $\hat{S}_\pm$ operators act on the state $|n,s\rangle$ as

$$\begin{aligned}&\hat{S}_-|n,s\rangle=f_{s,n}|n-1,s\rangle,\ \hat{S}_+|n,s\rangle=f_{s,n+1}|n+1,s\rangle,\\&\hat{S}_0|n,s\rangle=(n+s)|n,s\rangle,\ \hat{S}^2|n,s\rangle=s(s-1)|n,s\rangle,\end{aligned} \tag{5}$$

where $f_{s,n}=\sqrt{n(n+2s-1)}$ and $\hat{S}^2=\hat{S}_0^2-\frac{1}{2}(\hat{S}_+\hat{S}_-+\hat{S}_-\hat{S}_+)$, and where s is the Bargmann number.

In the case of an open cavity, the time evolution of the system under the damping is governed by the following master equation [50]:

$$\frac{\partial\rho(t)}{\partial t}=-i[\hat{H},\rho]+\gamma(2\hat{S}_-\rho\hat{S}_+-\hat{S}_+\hat{S}_-\rho-\rho\hat{S}_+\hat{S}_-), \tag{6}$$

where γ denotes the decay rate of the cavity mode. In the case of a high $-Q$ cavity $(\gamma\ll\lambda)$, analytical solutions for Eq. (6) can be obtained using the representation in the eigenstates of the Hamiltonian in Eq. (4) [10,51,52]. This representation is based on the complete set of the Hamiltonian eigenstates: $\{|\Psi_n^\pm\rangle\}$ with their eigenvalues $\{E_n^\pm\}$. In this representation, the SU(1, 1) system operators, $\hat{S}_\pm$ and $\hat{S}_+\hat{S}_-$, are rewritten in terms of the eigenstates $\{|\Psi_n^\pm\rangle\}$, using the transform,

$$\dot{Z}(t)=e^{i\hat{H}t}\frac{\partial\rho}{\partial t}e^{-i\hat{H}t}+i[\hat{H},Z(t)]. \tag{7}$$

Equation (6) then becomes

$$\begin{aligned}\dot{Z}(t)=&e^{i\hat{H}t}\gamma(2\hat{S}_-\hat{\rho}\hat{S}_+-\hat{\rho}\hat{S}_+\hat{S}_--\hat{S}_+\hat{S}_-\hat{\rho})e^{-i\hat{H}t}\\&=|0,g\rangle\langle 1,g|Z|1,g\rangle\langle 0,g|+|0,f\rangle\langle 1,f|Z|1,c\rangle\langle 0,f|\\&+2\gamma\sum_{m,n=1}^{\infty}f_{s,n+1}f_{s,m+1}\hat{K}_{11}+\frac{1}{4}\Lambda_{s,n}^+\Lambda_{s,m}^+(\hat{K}_{22}+\hat{K}_{33})\\&+\frac{1}{4}\Lambda_{s,n}^-\Lambda_{s,m}^-(\hat{K}_{23}|e^{2i(\mu_n-\mu_m)t}+\hat{K}_{32}e^{-2i(\mu_n-\mu_m)t})\\&-\gamma\sum_n f_{s,n+1}^2(Z\hat{G}_1^n+\hat{G}_1^nZ)+\frac{1}{2}(Z[\hat{G}_2^n+\hat{G}_3^n]\\&+[\hat{G}_2^n+\hat{G}_3^n]Z)F_{s,n},\end{aligned} \tag{8}$$

with

$$\Lambda_{s,n}^\pm=(f_{s,n}\pm f_{s,n+1}),\quad F_{s,n}=(f_{s,n}^2+f_{s,n+1}^2),$$

$\hat{K}_{rs}=|\Psi_r^{n-1}\rangle\langle\Psi_s^n|Z|\Psi_s^m\rangle\langle\Psi_r^{m-1}|$, and $\hat{G}_r=|\Psi_r^n\rangle\langle\Psi_r^n|$. To find the particular solution of the density matrix $\tilde{\rho}(t)$, we consider that the SU(3) system is initially in its upper state, $\hat{\rho}_a(0) = |e\rangle\langle e|$, while the two-mode cavity is initially in the superposition of BGCSs [34],

$$|\psi_c(0)\rangle = \frac{1}{A}[|\alpha, s\rangle + r|-\alpha, s\rangle] = \sum_{n=0}^{\infty} \frac{1}{A}\xi_n|n, s\rangle, \tag{9}$$

with

$$\xi_n = \alpha^n[1 + (-1)^n r]\sqrt{\frac{|\alpha|^{2s-1}}{n! I_{2s-1}(2|\alpha|)\Gamma(2s+n)}}, \tag{10}$$

where $|\alpha, s\rangle$ is the eigenstate of the lowering operator S_-; and $\hat{S}_-|\alpha, s\rangle_{BG} = \alpha|\alpha, s\rangle_{BG}$, a state that is also known as the Bergmann coherent state. $I_\nu(x)$ is the first kind modified Bessel function, and $A = 1 + r^2 + 2\langle\alpha, s|-\alpha, s\rangle$. If $r = 0$, we get the BGCS while the even BGCS is obtained for $r = 1$. The BGCSs were constructed for charge carriers in anisotropic $2D$ Dirac materials immersed in a constant homogeneous magnetic field [38]. The BGCSs correspond to the even and odd coherent states for $s = \frac{1}{4}$ and $s = \frac{3}{4}$, respectively. If $s = \frac{1}{2}$, a nonlinear coherent state $|\alpha, \frac{1}{2}\rangle$ can be driven from the BGCS, which was realized by a trapped ion [53] and photonic lattices [54].

By using Eq. (8) and the initial density matrix $\rho(0) = Z(0)$ in the eigenstates basis: $\{|\Psi_n^{\pm}\rangle\}$, the off-diagonal nonzero elements of the density matrix $Z(t)$, for $i \neq j$, are given by

$$Z_{i,j}^{mn}(t) = \langle\Psi_m^i|Z(t)|\Psi_n^j\rangle = \frac{1}{2}\xi_i\xi_j^* e^{-\frac{\gamma}{2}[F_{s,i}+F_{s,j}]t}. \tag{11}$$

The dynamics of the diagonal elements $Z_i^{mn}(t)$ verify

$$\dot{Z}_i^{11}(t) = 2\gamma f_{s,i+2}^2 Z_{i+1}^{11}(t) - 2\gamma f_{s,i+1}^2 Z_i^{11}(t),$$

$$\dot{Z}_i^{22}(t) = \frac{\gamma}{2}\chi_+ Z_{i+1}^{22}(t) + \frac{\gamma}{2}\chi_- Z_{i+1}^{33}(t) - \gamma F_{s,i} Z_i^{22}(t),$$

$$\dot{Z}_i^{33}(t) = \frac{\gamma}{2}\chi_+ Z_{i+1}^{33}(t) + \frac{\gamma}{2}\chi_- Z_{i+1}^{22}(t) - \gamma F_{s,i} Z_i^{33}(t),$$

where $\chi_\pm = (f_{s,i+2} \pm f_{s,i+1})^2$. After determining the elements of the matrix $Z(t)$, we use the inverse canonical transformation $\rho(t) = e^{-i\hat{H}t}Z(t)e^{i\hat{H}t}$. In the basis space states $\{|1\rangle_n = |e, n, s\rangle, |1\rangle_n = |g, n+1, s\rangle, |1\rangle_n = |f, n+1, s\rangle\}$, the density matrix $\rho(t)$ takes the form

$$\hat{\rho}(t) = \sum_{m,n=0}^{\infty} \sum_{k,j=1,2,3} \rho_{mn}|k\rangle_{mn}\langle j|,$$

$$\rho_{mn} = \langle m; s|e^{-i\hat{H}t}Z(t)e^{i\hat{H}t}|n; s\rangle. \tag{12}$$

This expression will be used to study the dynamics of the considered system.

A. Population Inversion of the Λ-Type System

The population inversion of the Λ-type system is used as an indicator of quantum coherence and the energy transition between its states. Its quantifier is based on the difference between the expected values of finding the system in its excited $|e\rangle$ and its ground states $|g\rangle + |f\rangle$. Based on the elements of the reduced density matrix of the system, the SU(3) system population takes the form

$$W(t) = \rho_{aa}(t) - [\rho_{bb}(t) + \rho_{cc}(t)]. \tag{13}$$

The appearance of the revival intervals of the atomic inversion is an interesting phenomenon. It is a good indicator of the quantum coherence, which is generated due to the unitary SU(3)–SU(1, 1) interaction between the two-mode cavity fields and the three-level atom.

B. Von Neumann Entropy

Generally, in the absence of the decoherence/dissipation, the von Neumann entropy and its partial functions are used to quantify the SU(3)–SU(1, 1) entanglement. While in the presence of the decoherence/dissipation, the total entropy is time-independent. The partial entropies of the SU(1, 1) and SU(3) systems quantify the mixedness (coherence loss) of the two-mode cavity fields and the Λ-type three-level atom, respectively [55–58].

The SU(3)–SU(1, 1) entropy is given by

$$E(t) = -\sum_{k=1} \lambda_k \ln \lambda_k, \tag{14}$$

where λ_k are the eigenvalues of the total system density matrix $\hat{\rho}(t)$. By using the eigenvalues of the reduced density matrices π_n^i of the atomic system $\rho^A(t)$, and of the two-mode field $\rho^F(t)$, where $\rho^{A(F)}(t) = Tr_{F(A)}(\hat{\rho}(t))$, the entropy functions of the atomic system and the cavity are given by

$$E_i(t) = -\sum_{n=1} \pi_n^i \ln \pi_n^i, \quad i = A, F. \tag{15}$$

The von Neumann entropy and its partial entropies satisfy the inequality of Araki–Lieb that is given by [59]

$$|E_A(t) - E_F(t)| \leq E(t) \leq E_A(t) + E_F(t). \tag{16}$$

For pure state and without damping, the SU(3)–SU(1, 1) entropy is time-independent; $E(t) = 0$. Consequently, according to the Araki–Lieb inequality, $E_A(t) = E_F(t)$. Only one of them is needed to measure the mixedness and entanglement for any subsystems. In this case, the mixedness and the entanglement have the same dynamical behavior. However, in the case of initial mixed states with damping, the SU(3)–SU(1, 1) entropy is time-dependent $E(t) \neq 0$ and $E_A(t) \neq E_F(t)$. In this case, the entropy functions grow as the time evolves.

By using the analytical solutions in Eq. (12), we present here the numerical calculations for the three-level system of Λ-type for different cases of the Barut–Girardello states: $r = 0$ and $r = 1$ in the presence and absence of dissipation.

In Figs. 1–3, we draw the population inversion $W(t)$, the entropies of the system $E(t)$, the SU(3) system $E_A(t)$, and of the SU(3) system $E_F(t)$ when the two-mode cavity is initially in a superposition of the Barut–Girardello states with $r = 0$ (B-GCS) in Figs. 1 and 3 and $r = 1$ (even BGCS) in Fig. 2. The dissipation effect is shown in Figs. 1(b), 2(b), and 3(b).

Figure 1(a) illustrates the time-evolution of the population inversion, the SU(3) and SU(1, 1) entropies ($E_A(t)$, $E_F(t)$) as well as the SU(3)–SU(1, 1) entropy without the dissipation

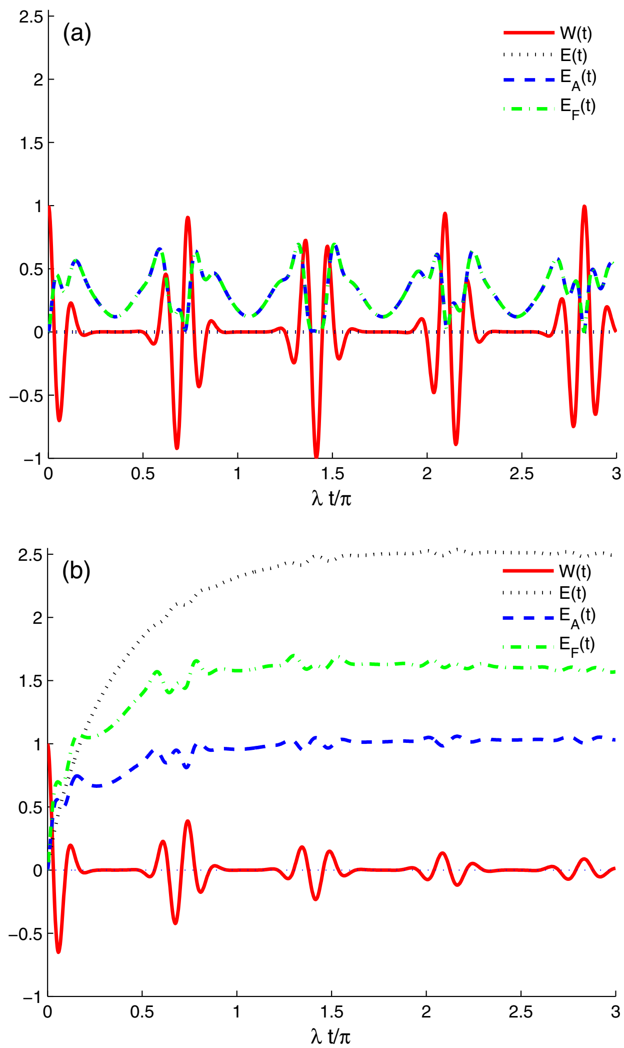

Fig. 1. Dynamics of the population inversion and the entropies for $s = \frac{1}{4}$, $r = 0$, and $\alpha = 5$ with different dissipation values: (a) $\gamma = 0$ and (b) $\gamma = 0.007\lambda$.

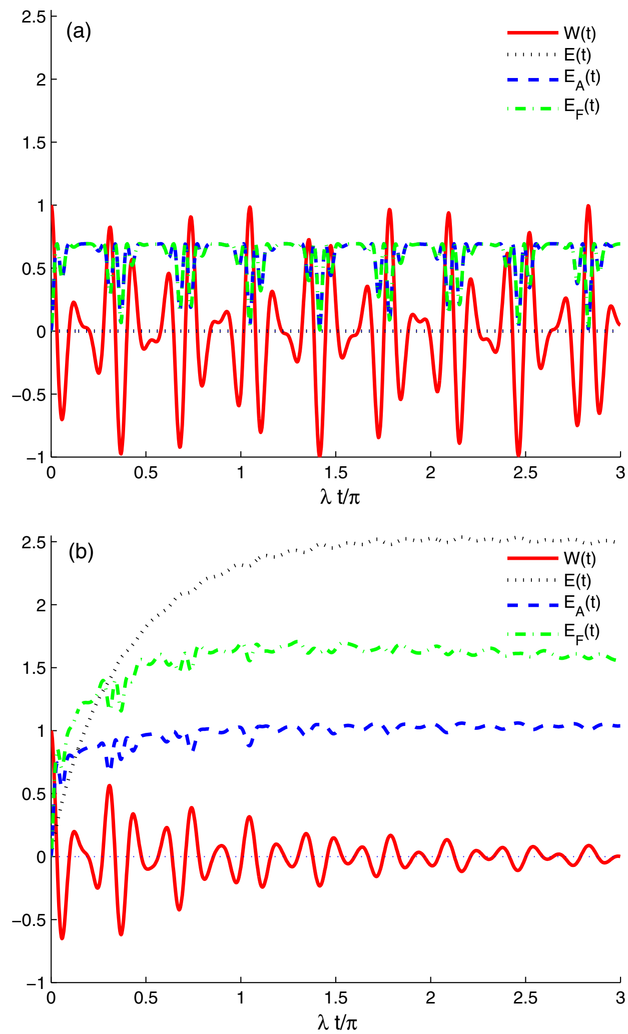

Fig. 2. Dynamics of the population inversion and the entropies of Fig. 1 ($s = \frac{1}{4}$ and $\alpha = 5$), but for the initial even BGCS.

effect. The population inversion fluctuates between its maxima and minima ± 1, which corresponds to the upper and lower states (see solid curve). The $W(t)$ has regular oscillations due to the unitary interaction, while both $E_A(t)$ and $E_F(t)$ have the same dynamics that fluctuate between zero and the maximum while $E(t) = 0$, as expected. The partial entropies $E_A(t)$ and $E_F(t)$ have minimum and maximum values at the revivals of the population inversion. This indicates that the field does not return to its initial state at $\lambda t = 0$.

While the picture is completely different in Fig. 1(b) due to the dissipation, the states of the qutrit-cavity, the qutrit, and the cavity field evolve from a pure state at $\lambda t = 0$ to a statistical mixture. This is in concordance with Fig. 1(b), where we note that the entropy of the total system $E(t)$ increases monotonically and no longer equals zero, while the partial entropies $E_A(t)$ and $E_F(t)$ are no longer equal. Also, we note that the revivals of the population inversion disappear completely after a short time. However, due to the dissipation, the entropies increase monotonically. After a short time ($\lambda t < 0.3$), the entropy of the total system $E(t)$ attains higher values than the partial entropies, while $E_F(t)$ is always higher than $E_A(t)$ for any value of γ.

To analyze the influence of the even BGCS $|\psi(0)\rangle = \frac{1}{A}[|\alpha, s\rangle + r| - \alpha, s\rangle]$, we plot in Fig. 2 the population inversion $W(t)$ and the partial entropies ($E_A(t)$, $E_F(t)$) as well as the total entropy $E(t)$ for even BGCS ($r = 1$) with the same parameter values as in Fig. 1. The entropies evolutions are quite changed when we treat an even BGCS. We observe higher frequency oscillations compared to the cases of Fig. 1. In Fig. 2(a), $\gamma = 0$, and we notice that both partial entropies $E_A(t)$ and $E_F(t)$ present the same behavior, so $E(t) = 0$. The field and the particle are strongly entangled at all times except at the revival time, which could be explained in the next section by observing the plots of the negativity and mutual information, as shown in Fig. 5(a).

The dissipation effect shown in Fig. 2(b) leads to more rapid suppression of the generated quantum coherence. The entropies $E_F(t)$ and $E(t)$ grow, while $E_A(t)$ converges to a steady-state value as time evolves [see Fig. 2(b)].

To investigate the influence of the two-mode field intensities on the degree of entanglement, and the quantum correlation, we plot the functions $W(t)$, $E_A(t)$, and $E_F(t)$ as well as $E(t)$

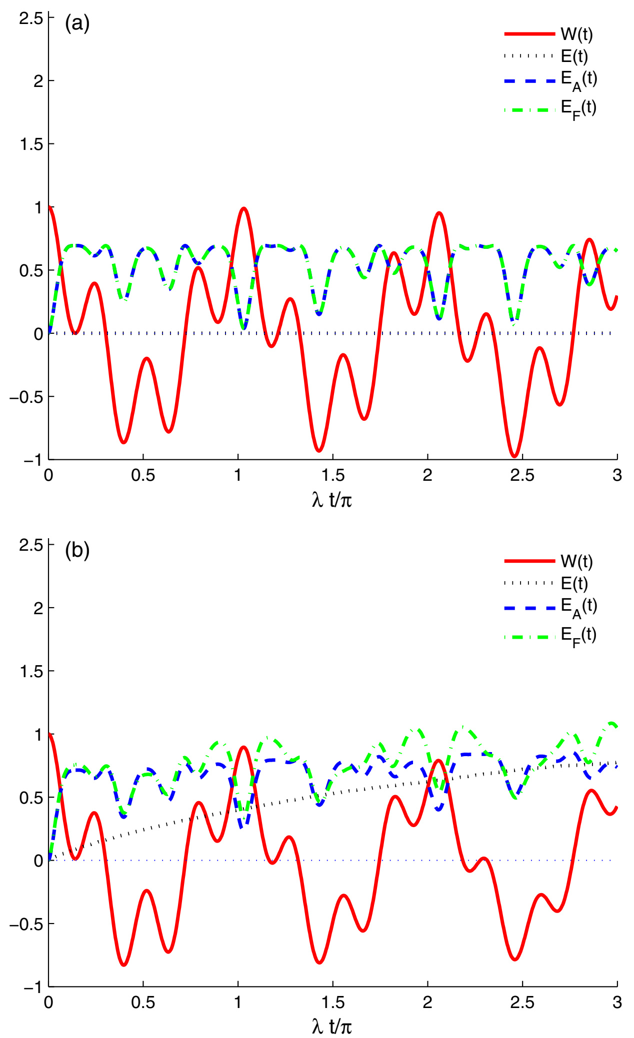

Fig. 3. Dynamics of the population inversion and the entropies of Fig. 2 ($s = \frac{1}{4}$ and $r = 1$), but for small initial coherent intensity $\alpha = 1$.

in Fig. 3 using the same parameters values as of Fig. 1 but for $\alpha = 1$. Here, the dynamics of the population inversion and the quantum coherence changes completely. In Fig. 3, the entropies have irregular maxima/minima, which corresponds to quasi-regular population inversion revivals. For the even coherent state with small mean photon values, the partial entropies $E_A(t)$ and $E_F(t)$ present the same behavior while the total entropy $E(t)$ vanishes ($E(t) = 0$) [see Fig. 2(a)]. The qutrit-cavity entanglement is higher than the case of large values of the two-mode field intensities. We conclude that the photon number plays an important role in the generation of the entanglement between the SU(3) and SU(1, 1) systems.

Figure 3(b) shows the dissipation effect on the population inversion and the entropies for small two-mode field intensities. By comparing these curves to the plots obtained in Fig. 2(b), we deduce that the dynamics of the population inversion and the quantum coherence of the qutrit-cavity system and its subsystems are more robust against the dissipation in the case of a small initial coherent intensity.

3. NEGATIVITY AND MUTUAL ENTROPY DYNAMICS

For the mixed states, the total system entropy is time-dependent $E(t) \neq 0$, and the partial entropies are different and do not give the same information. In this case, the entropy functions are only used to display the mixedness, and to quantify the quantum correlation between the parts of the system. We use the negativity in addition to the mutual entropy as a measure of the system total correlation.

- Based on the negative eigenvalues μ_k of the partial transpose of the density matrix, the negativity [60] is given by

$$N(t) = -\sum_k \mu_k. \tag{17}$$

If $N(t) = 0.5$, then the system is in a maximally entangled state. $N(t) = 0$ indicates that the system is a pure state. Otherwise, if $0 < N(t) < 0.5$, then the atom–cavity interaction presents partial entanglement.

- The mutual entropy is used to quantify the total correlation (quantum and classical) in the system, and is given by [61]

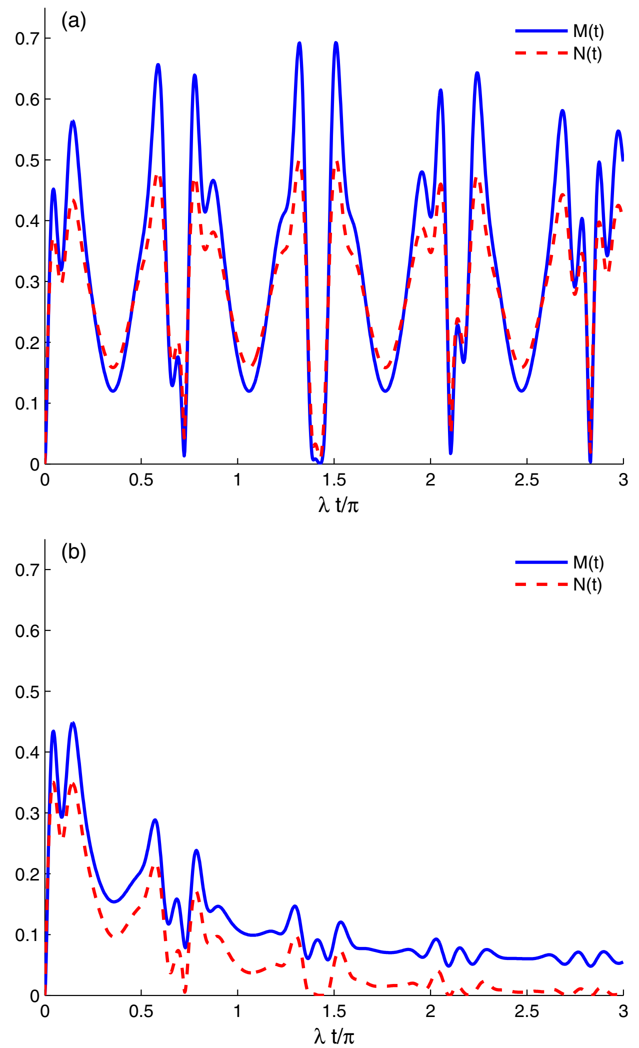

Fig. 4. Dynamics of the negativity and the mutual entropy for $s = \frac{1}{4}$ and $\alpha = 5$, and the initial BGCS with different dissipation values: (a) $\gamma = 0.0$ and (b) $\gamma = 0.01\lambda$.

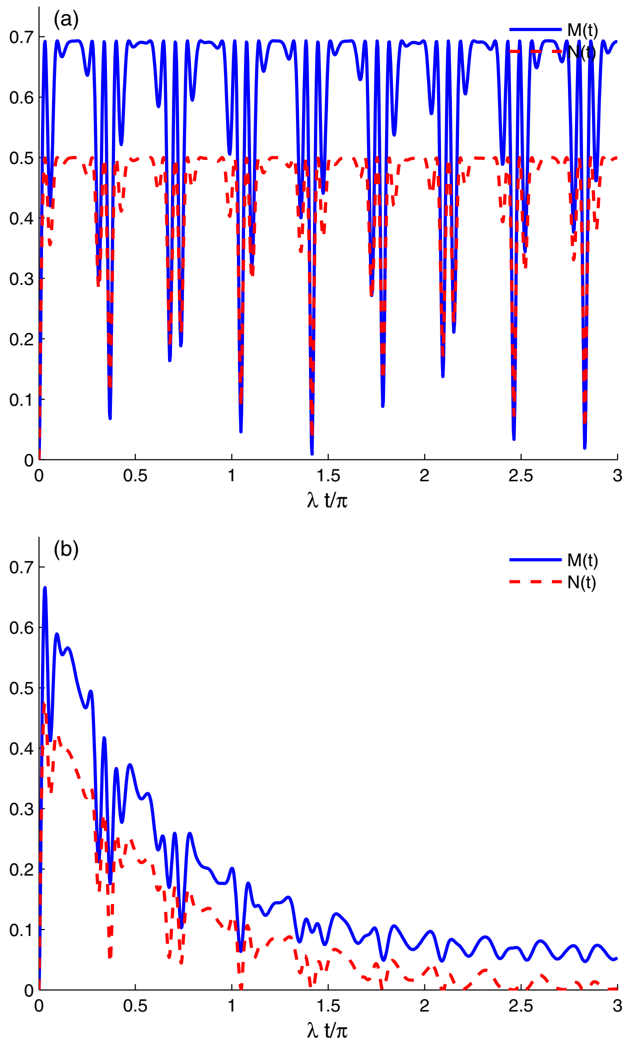

Fig. 5. Dynamics of the negativity and the mutual entropy of Fig. 4 ($s = \frac{1}{4}$ and $\alpha = 5$), but for the initial even BGCS $r = 1$.

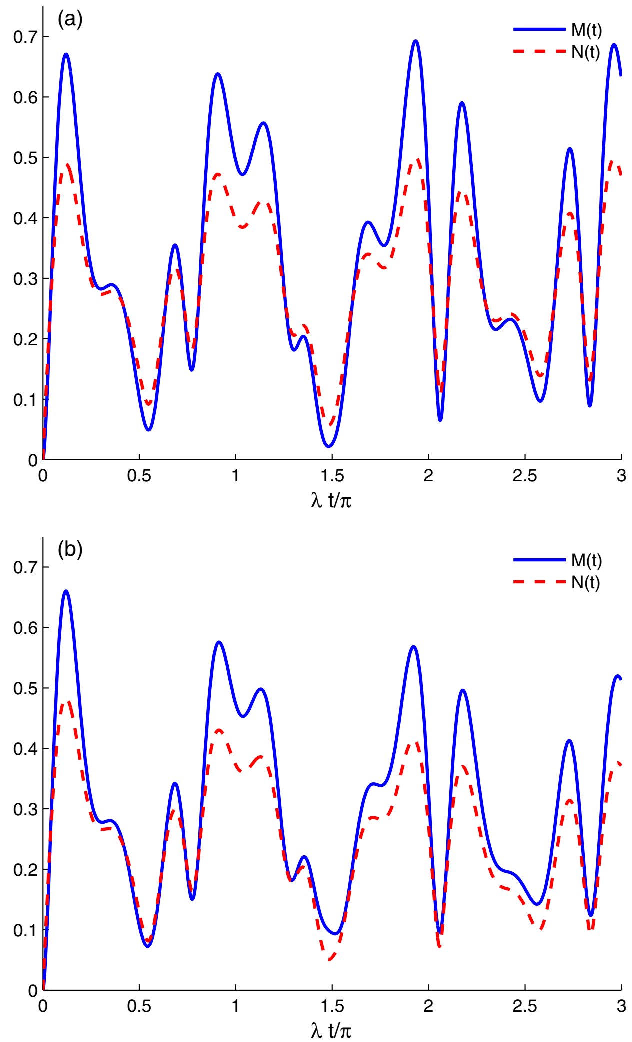

Fig. 6. Dynamics of the negativity and the mutual entropy of Fig. 4 ($s = \frac{1}{4}$ and $r = 0$), but for small initial coherent intensity $\alpha = 1$.

$$M(t) = \frac{1}{2}[E_A(t) + E_F(t) - E(t)]. \quad \textbf{(18)}$$

If $M(t) = 0$, the qutrit-cavity state is an uncorrected state; however, if $M(t) \neq 0$, then it shows partial and maximal correlations in the system.
The mutual entropy can also be used as a useful order parameter for quantum synchronization between the SU(3) and SU(1, 1) subsystems [62,63]. Therefore, there is a relation between the synchronization and the correlations [64,65].

In Figs. 4–6, we investigate dynamics of the entanglement, the synchronization, and the total correlation between the qutrit-cavity subsystems for different cases of the initial coherent cavity states, $r = 0$ (BGCS) and $r = 1$ even BGCS, in the presence and absence of the dissipation effect.

Figure 4 shows the negativity $N(t)$ (lower dashed curve) compared to the mutual entropy $M(t)$ (upper solid curve) with the initial BGCS for $\gamma = 0$ in Fig. 4(a) and $\gamma = 0.01$ in Fig. 4(b). As shown in Fig. 4(a), the negativity $N(t)$ and the mutual entropy $M(t)$ present the same behavior. They have minima at the population inversion revivals, and the decay process takes place in the population inversion collapse region. Note that, in the absence of the dissipation, the quantum synchronization and entanglement between the subsystems have the same dynamical behavior, which means that the synchronization can be considered an indicator of the generated quantum correlations [65,66]. The effect of the dissipation on the synchronization and entanglement is shown for $\gamma = 0.01$ in Fig. 4(b). The negativity and the mutual entropy amplitudes are heavily affected by the dissipation. The reduction of the mutual entropy synchronization is due to the fact that the mutual entropy depends on the subsystem entropies that have different dynamic behavior in the presence of the dissipation.

Figure 5 shows the effect of the even BGCS on the dynamics of the synchronization and the correlations of $N(t)$ and $M(t)$, which are generated due to the qutrit-cavity evolution in the presence and absence of dissipation. The values of the maxima and minima of the negativity as well as the mutual entropy are enhanced. This mean that the high nonclassicality of the initial even Barut–Girardello coherent state enhances the generated synchronization and the correlations. In Fig. 5(b), where we consider the dissipation for the initial even Barut–Girardello coherent state, the synchronization and the correlation deteriorate. The synchronization is more robust against the dissipation than the generated correlations.

In Fig. 6, we illustrate the effect of the initial coherent intensity of the two-mode cavity field on the synchronization and the correlation functions. For a small coherent intensity, the functions $N(t)$ and $M(t)$ present a strong synchronization and entanglement. By comparing the plots of Figs. 6 and 4, we find that, for a small value of α, the dissipation effect on the synchronization and entanglement is reduced. The robustness of the generated synchronization and entanglement against the dissipation is enhanced when the initial coherent mode field intensities decrease. The generation and the robustness of the quantum synchronization as well as the correlations between the subsystems depend on the initial cavity field states and the dissipation.

4. CONCLUSION

In the present paper, we have discussed the dynamics of a three-level atom Λ-type that resonantly interacts with an open bimodal cavity under dissipation. The analytical solution of the master equation is obtained when the two-mode cavity field is initially in a superposition of nonlinear BGCSs. The revivals and collapses of the population inversion are investigated under the effect of the initial cavity field states and the dissipation. The dynamics of the entropy are used to explore the generated entanglement (if the dissipation is absent) and the mixedness (in the presence of the dissipation). For two cases of the initial BGCSs, we discuss the generation and the robustness of the quantum synchronization and the correlations between the subsystems by using the negativity and the mutual entropy. It is found that the dynamics of the quantum synchronization and the correlations are highly sensitive to the dissipation, the superposition, and the intensity of the initial BGCSs.

Acknowledgment. The authors are very grateful to the referees for their constructive remarks, which have helped to improve the paper.

Disclosures. The authors declare no conflicts of interest.

Data Availability. Data underlying the results presented in this paper are not publicly available at this time but may be obtained from the authors upon reasonable request.

REFERENCES

1. K. Heshami, D. G. England, P. C. Humphreys, P. J. Bustard, V. M. Acosta, J. Nunn, and B. J. Sussman, "Quantum memories: emerging applications and recent advances," J. Mod. Opt. **63**, 2005–2028 (2016).
2. A.-S. F. Obada, H. A. Hessian, and A.-B. A. Mohamed, "Output entanglement from SU(1, 1) coherent states under nonlinear dissipation in the dispersive limit," J. Phys. A Math. Theor. **43**, 025305 (2010).
3. A.-B. A. Mohamed, H. Eleuch, and C. H. Raymond Ooi, "Quantum coherence and entanglement partitions for two driven quantum dots inside a coherent micro cavity," Phys. Lett. A **383**, 125905 (2019).
4. A.-B. A. Mohamed, H. Eleuch, and C. H. Raymond Ooi, "Non-locality correlation in two driven qubits inside an open coherent cavity: trace norm distance and maximum bell function," Sci. Rep. **9**, 19632 (2019).
5. C. H. Bennett, G. Brassard, C. Crépeau, R. Jozsa, A. Peres, and W. K. Wootters, "Teleporting an unknown quantum state via dual classical and Einstein-Podolsky-Rosen channels," Phys. Rev. Lett. **70**, 1895 (1993).
6. K. Mattle, H. Weinfurter, P. G. Kwiat, and A. Zeilinger, "Dense coding in experimental quantum communication," Phys. Rev. Lett. **76**, 4656 (1996).
7. K. Ekert, "Quantum cryptography based on Bell's theorem," Phys. Rev. Lett. **67**, 661 (1991).
8. R. Raussendorf and H. J. Briegel, "A one-way quantum computer," Phys. Rev. Lett. **86**, 5188 (2001).
9. A.-S. F. Obada, H. A. Hessian, and A.-B. A. Mohamed, "Effects of cavity damping on the entanglement for a three-level atomic system," J. Mod. Opt. **56**, 881–885 (2009).
10. S. M. Barnett and P. L. Knight, "Dissipation in a fundamental model of quantum optical resonance," Phys. Rev. A **33**, 2444 (1986).
11. R. R. Puri and G. S. Agarwal, "Finite-*Q* cavity electrodynamics: dynamical and statistical aspects," Phys. Rev. A **35**, 3433 (1987).
12. A.-S. F. Obada, H. A. Hessian, and A.-B. A. Mohamed, "The effects of thermal photons on entanglement dynamics for a dispersive Jaynes–Cummings model," Phys. Lett. A **372**, 3699 (2008).
13. A.-B. A. Mohamed and H. Eleuch, "Generation and robustness of bipartite non-classical correlations in two nonlinear microcavities coupled by an optical fiber," J. Opt. Soc. Am. B **35**, 47–53 (2018).
14. A.-B. A. Mohamed, A. H. Homid, M. Abdel-Aty, and H. Eleuch, "Trace-norm correlation beyond entanglement in InAs nanowire system with spin–orbit interaction and external electric field," J. Opt. Soc. Am. B **36**, 926–934 (2019).
15. Q. A. Turchette, C. S. Wood, B. E. King, C. J. Myatt, D. Leibfried, W. M. Itano, and D. J. Wineland, "Deterministic entanglement of two trapped ions," Phys. Rev. Lett. **81**, 3631 (1998).
16. J. Q. You, "Cooper-pair-box qubits in a quantum electrodynamic cavity," Phys. E **18**, 33–34 (2003).
17. J. Q. You and F. Nori, "Quantum information processing with superconducting qubits in a microwave field," Phys. Rev. B **68**, 064509 (2003).
18. E. T. Jaynes and F. W. Cummings, "Comparison of quantum and semiclassical radiation theories with application to the beam maser," Proc. IEEE **51**, 89–109 (1963).
19. A. M. Abdel-Hafez, A.-S. F. Obada, and M. M. A. Ahmad, "*N*-level atom and *N-1* modes: statistical aspects and interaction with squeezed light," Phys. Rev. A **35**, 1634 (1987).
20. M. Ghasemi, M. K. Tavassoly, and A. Nourmandipour, "Dissipative entanglement swapping in the presence of detuning and Kerr medium: Bell state measurement method," Eur. Phys. J. Plus **132**, 531 (2017).
21. X. Zou, K. Pahlke, and W. Mathis, "Generation of an entangled state of two three-level atoms in cavity QED," Phys. Rev. A **67**, 044301 (2003).
22. H. Tan, H. Xia, and G. Li, "Interference-induced enhancement of field entanglement from an intracavity three-level V-type atom," Phys. Rev. A **79**, 063805 (2009).
23. D. Kaszlikowski, P. Gnaciéski, M. Żukowski, W. Miklaszewski, and A. Zeilinger, "Violations of local realism by two entangled *N*-dimensional systems are stronger than for two qubits," Phys. Rev. Lett. **85**, 4418 (2000).
24. D. Bruss and C. Macchiavello, "Optimal eavesdropping in cryptography with three-dimensional quantum states," Phys. Rev. Lett. **88**, 127901 (2002).
25. P. B. Dixon, G. A. Howland, J. Schneeloch, and C. Howell, "Quantum mutual information capacity for high-dimensional entangled states," Phys. Rev. Lett. **108**, 143603 (2012).
26. Z. B. Feng, R. Y. Yan, and Y. Q. Zhou, "Quantum state transfer with a two-dimensional Cooper-pair box qubit array," Quantum Inf. Transition **12**, 1429–1438 (2013).
27. S. K. Mishra, L. Chotorlishvili, A. R. P. Rau, and J. Berakdar, "Three-level spin system under decoherence-minimizing driving fields: application to nitrogen-vacancy spin dynamics," Phys. Rev. A **90**, 033817 (2014).
28. A. H. Gharamalekia, A. Kevin, and M. A. T. G. Jahani, "Light drag via electron tunneling and incoherent pumping in semiconductor three-level InAs/GaAs double quantum dot molecules," Eur. Phys. J. D **73**, 257 (2019).
29. C. Li, S. Yang, J. Song, Y. Xia, and W. Ding, "Generation of long-living entanglement between two distant three-level atoms in

non-Markovian environments," Opt. Express **25**, 10961–10971 (2017).
30. M. R. Abbasi, "Thermal free entanglement of a Λ-type three-level atom and bimodal photons in an optical cavity," Physica A **545**, 123424 (2020).
31. M. Miranda and M. Orszag, "Control of interference and diffraction of a three-level atom in a double-slit scheme with cavity fields," Phys. Rev. A **102**, 033723 (2020).
32. H. Azuma, "Numerical analyses of emission of a single-photon pulse based on single-atom–cavity quantum electrodynamics," Prog. Theor. Exp. Phys. **2019**, 063A01 (2019).
33. N. Shirkhanghah, M. Saadati-Niari, and S. Ahadpour, "Fractional population transfer among three-level systems in a cavity by Stark-shift-chirped rapid adiabatic passage," Quantum Inf. Process. **19**, 128 (2020).
34. A. O. Barut and L. Girardello, "New "coherent" states associated with non-compact groups," Commun. Math. Phys. **21**, 41–55 (1971).
35. C. H. Bennett, P. W. Shor, J. A. Smolin, and A. V. Thapliyal, "Entanglement-assisted classical capacity of noisy quantum channels," Phys. Rev. Lett. **83**, 3081 (1999).
36. G. S. Agarwal, "Nonclassical statistics of fields in pair coherent states," J. Opt. Soc. Am. B **5**, 1940–1947 (1988).
37. X. G. Wang, "Two-mode nonlinear coherent states," Opt. Commun. **178**, 365–369 (2000).
38. Y. Concha-Sánchez, E. Díaz-Bautista, and A. Raya, "Barut–Girardello coherent states for anisotropic 2D-Dirac materials," J. Phys. Condens. Matter **31**, 435702 (2019).
39. F. Jahanbakhsh and M. K. Tavassoly, "The field-field and dipole-dipole coupling effects on the entanglement of the interaction between two qutrits with a two-mode field," Mod. Phys. Lett. A **35**, 22050183 (2020).
40. N. H. Abd El-Wahab, A. S. Abdel Rady, A.-N. A. Osman, and A. Salah, "Dynamics of three-level Λ-type atom interacting with one mode cavity field with both classical gravity and quantum radiation: Lie algebra approach," Eur. Phys. J. Plus **130**, 207 (2015).
41. M. Ghorbani, H. Safari, and M. J. Faghihi, "Controlling the entanglement of a Λ-type atom in a bimodal cavity via atomic motion," J. Opt. Soc. Am. B **33**, 1022–1029 (2016).
42. W. L. Yang, Z. Q. Yin, Z. Y. Xu, M. Feng, and C. H. Oh, "Quantum dynamics and quantum state transfer between separated nitrogen-vacancy centers embedded in photonic crystal cavities," Phys. Rev. A **84**, 043849 (2011).
43. Z.-B. Feng and X.-J. Lu, "Optimal controls of invariant-based population transfer in a superconducting qutrit," Quantum Inf. Process. **19**, 83 (2020).
44. C.-P. Yang, S.-I. Chu, and S. Han, "Quantum information transfer and entanglement with SQUID qubits in cavity QED: a dark-state scheme with tolerance for nonuniform device parameter," Phys. Rev. Lett. **92**, 117902 (2004).
45. A. F. Kockum, A. Miranowicz, V. Macri, S. Savasta, and F. Nori, "Deterministic quantum nonlinear optics with single atoms and virtual photons," Phys. Rev. A **95**, 063849 (2017).
46. C. Liu, J. F. Chen, S. Zhang, S. Zhou, Y.-H. Kim, M. M. T. Loy, G. K. L. Wong, and S. Du, "Two-photon interferences with degenerate and nondegenerate paired photons," Phys. Rev. A **85**, 021803 (2012).
47. H. I. Yoo and J. H. Eberly, "Dynamical theory of an atom with two or three levels interacting with quantized cavity fields," Phys. Rep. **118**, 239–337 (1985).
48. C. C. Gerry, "Two-photon Jaynes-Cummings model interacting with the squeezed vacuum," Phys. Rev. A **37**, 2683 (1988).
49. M. Ban, "Decomposition formulas for su(1, 1) and su(2) Lie algebras and their applications in quantum optics," J. Opt. Soc. Am. B **10**, 1347–1359 (1993).
50. W. P. Schleich, *Quantum Optics in Phase Space* (Wiley-VCH, 2001).
51. A.-S. F. Obada, H. A. Hessian, and A.-B. A. Mohamed, "Entropies and entanglement for decoherence without energy relaxation in a two-level atom," J. Phys. B **40**, 2241 (2007).
52. A.-B. A. Mohamed and H. Eleuch, "Coherence and information dynamics of a Λ-type three-level atom interacting with a damped cavity field," Eur. Phys. J. Plus **132**, 75 (2017).
53. R. L. de Matos Filho and W. Vogel, "Nonlinear coherent states," Phys. Rev. A **54**, 4560 (1996).
54. S. Dehdashti, R. Li, J. Liu, F. Yu, and H. Chen, "Realization of non-linear coherent states by photonic lattices," AIP Adv. **5**, 067165 (2015).
55. S. J. D. Phoenix and P. L. Knight, "Establishment of an entangled atom-field state in the Jaynes-Cummings model," Phys. Rev. A **44**, 6023 (1991).
56. A.-S. F. Obada, H. A. Hessian, and A.-B. A. Mohamed, "Influence of phase damping on the entanglement for the damped JC model in the pure and mixed states," Laser Phys. **18**, 1111–1117 (2008).
57. A.-S. F. Obada, F. A. Mohammed, H. A. Hessian, and A.-B. A. Mohamed, "Entropies and entanglement for initial mixed state in the multi-quanta JC model with the Stark shift and Kerr-like medium," Int. J. Theor. Phys. **46**, 1027–1044 (2007).
58. A.-S. F. Obada, H. A. Hessian, and A.-B. A. Mohamed, "Effect of phase-damped cavity on dynamics of tangles of a nondegenerate two-photon JC model," Opt. Commun. **281**, 5189–5193 (2008).
59. H. Araki and E. Lieb, "Entropy inequalities," Commun. Math. Phys. **18**, 160–170 (1970).
60. G. Vidal and R. F. Werner, "Computable measure of entanglement," Phys. Rev. A **65**, 032314 (2002).
61. S. M. Barnett and S. J. D. Phoenix, "Entropy as a measure of quantum optical correlation," Phys. Rev. A **40**, 2404 (1989).
62. V. Ameri, M. Eghbali-Arani, A. Mari, A. Farace, F. Kheirandish, V. Giovannetti, and R. Fazio, "Mutual information as an order parameter for quantum synchronization," Phys. Rev. A **91**, 012301 (2015).
63. W. Li, W. Zhang, C. Li, and H. Song, "Properties and relative measure for quantifying quantum synchronization," Phys. Rev. E **96**, 012211 (2017).
64. H. Eneriz, D. Z. Rossatto, F. A. Cárdenas-López, E. Solano, and M. Sanz, "Degree of quantumness in quantum synchronization," Sci. Rep. **9**, 19933 (2019).
65. T. Huan, R. Zhou, and H. Ian, "Synchronization of two cavity-coupled qubits measured by entanglement," Sci. Rep. **10**, 12975 (2020).
66. S. Siwiak-Jaszek, T. P. Le, and A. Olaya-Castro, "Synchronization phase as an indicator of persistent quantum correlations between subsystems," Phys. Rev. A **102**, 032414 (2020).